The Relationship between Membrane Fluidity and Permeabilities to Water, Solutes, Ammonia, and Protons

MARC B. LANDE,* JOANNE M. DONOVAN,‡ and MARK L. ZEIDEL§

From the *Childrens Hospital and Harvard Medical School, Boston, Massachusetts 02132; ‡Brockton-West Roxbury DVAMC, Boston, Massachusetts 02132; and §Laboratory of Epithelial Cell Biology, Renal Electrolyte Division, University of Pittsburgh Medical Center, Pittsburgh, Pennsylvania 15213

ABSTRACT Several barrier epithelia such as renal collecting duct, urinary bladder, and gastric mucosa maintain high osmotic pH and solute gradients between body compartments and the blood by means of apical membranes of exceptionally low permeabilities. Although the mechanisms underlying these low permeabilities have been only poorly defined, low fluidity of the apical membrane has been postulated. The solubility diffusion model predicts that lower membrane fluidity will reduce permeability by reducing the ability of permeant molecules to diffuse through the lipid bilayer. However, little data compare membrane fluidity with permeability properties, and it is unclear whether fluidity determines permeability to all, or only some substances. We therefore studied the permeabilities of a series of artificial large unilamellar vesicles (LUV) of eight different compositions, exhibiting a range of fluidities encountered in biological membranes. Cholesterol and sphingomyelin content and acyl chain saturation were varied to create a range of fluidities. LUV anisotropy was measured as steady state fluorescence polarization of the lipophilic probe DPH. LUV permeabilities were determined by monitoring concentration-dependent or pH-sensitive quenching of entrapped carboxyfluorescein on a stopped-flow fluorimeter. The relation between DPH anisotropy and permeability to water, urea, acetamide, and NH3 was well fit in each instance by single exponential functions ($r > 0.96$), with lower fluidity corresponding to lower permeability. By contrast, proton permeability correlated only weakly with fluidity. We conclude that membrane fluidity determines permeability to most nonionic substances and that transmembrane proton flux occurs in a manner distinct from flux of other substances.

INTRODUCTION

Several epithelial apical membranes such as those of the renal collecting duct and thick ascending limb, urinary bladder, and stomach exhibit strikingly low permeabilities to water and small nonelectrolytes such as urea (Kikeri, Sun, Zeidel, and

Address correspondence to Mark L. Zeidel, Laboratory of Epithelial Cell Biology, Renal Electrolyte Division, University of Pittsburgh Medical Center, Pittsburgh, PA 15213.

J. GEN. PHYSIOL. © The Rockefeller University Press · 0022-1295/95/07/67/23 $2.00
Volume 106 July 1995 67–84

Hebert, 1989; Harris, Strange, and Zeidel, 1991; Grossman, Harris, Star, and Zeidel, 1992; Priver, Rabon, and Zeidel, 1993; Zeidel, Strange, Emma, and Harris, Jr., 1993). Although these permeabilities have been measured in a number of biological membranes, the mechanisms by which these low permeability membranes function to limit the rate of flux remain unclear. In the absence of carrier molecules or channels, permeation of molecules across membranes is thought to occur via the lipid bilayer by a three-step process involving the partitioning of the substance from the aqueous phase on one side into the bilayer, its diffusion across the bilayer, and its partitioning from the bilayer into the aqueous phase on the other side (Finkelstein, 1986; Stein, 1989, 1990). This model, called the solubility-diffusion model of permeation, has been validated by the demonstration that the permeability of a substance is directly related to its oil-water partition coefficient, as well as to molecular radius, which provides a measure of the barrier to diffusion of the substance through the lipid bilayer itself (Finkelstein, 1986; Lieb, and Stein, 1969; Stein, 1989). The solubility-diffusion model also predicts that reductions in the fluidity of the lipid bilayer will reduce the rate at which substances diffuse across the bilayer (Finkelstein, 1986). Although some studies have related predicted membrane fluidity to water permeability (Finkelstein, 1986), there has been no systematic study comparing measured fluidities to measured permeabilities for a wide variety of membranes. We therefore investigated the relationship between averaged fluidity of the bilayer as estimated by DPH anisotropy and permeability by comparing permeabilities to water, urea, acetamide, ammonia, and protons (although it is not known at physiological pH levels whether protons cross the membrane in the form of H^+ (H_3O^+) or OH^-, we will use the term "protons" to refer to these fluxes) of a series of artificial lipid membranes (large unilamellar vesicles, LUV) exhibiting a wide range of fluidities. The results demonstrate a tight relationship between membrane fluidities and permeabilities for all substances except protons, indicating that protons cross the membrane by mechanisms distinct from those for other substances.

MATERIALS AND METHODS

Materials

Carboxyfluorescein (CF) and 1,6-diphenyl-1,3,5-hexatriene (DPH) were obtained from Molecular Probes, Inc. (Eugene, OR). Anti-fluorescein antibody was prepared as described (Harris, Kikeri, Janoshazi, Solomon, and Zeidel, 1990). Urea was obtained from Bio Rad Laboratories (Richmond, CA). Cholesterol (CH), sphingomyelin (SPH), 1-palmitoyl-2-oleoyl lecithin (POPC), 1-palmitoyl-2-arachidonoyl lecithin (PAPC), and dilinoleoyl lecithin (DLPC) were obtained from Avanti Polar Lipids, Inc. (Alabaster, AL). All other chemicals were obtained from Sigma Chemical Co. (St. Louis, MO).

Solutions

NaCl buffer contained 0.15 M NaCl, and 0.01 M *N*-(2-hydroxyethyl)piperazine-*N'*-2-ethanesulfonic acid (HEPES; pH 7.5, 310 mOsm/kg). KCl buffer contained 0.15 M NaCl, 0.03 M KCl, and 0.01 M HEPES (pH 7.5, 340 mOsm/kg). Nonelectrolyte buffer contained 0.1 M NaCl, 0.343 M nonelectrolyte (urea or acetamide), and 0.01 M HEPES (pH 7.5, 560 mOsm/kg).

LUV Preparation and Characterization

LUV of the following lipid compositions were prepared, based on a previous study which developed algorithms for relating lipid composition to fluorescence anisotropy (Van Blitterswijk, Van Der Meer, and Hilkmann, 1987): (*a*) 100% DLPC; (*b*) 100% PAPC; (*c*) 100% POPC; (*d*) 90% POPC/10% CH M/M; (*e*) 80% POPC/20% CH; (*f*) 60% POPC/40% CH; (*g*) 25% POPC/35% SPH/40% CH; and(*h*) 60% SPH/40% CH. The appropriate lipids were mixed, dried under N2, and lyophilized to remove residual solvent. Lipid was then resuspended in NaCl buffer and LUV were made by serial extrusion of lipid through a polycarbonate filter (High Pressure Vesicle Extruder, Sciema, Vancouver, Canada; Nuclepore, 0.1 μm) (Priver et al., 1993.; Lande, Priver, and Zeidel, 1994). CF was added to buffer before extrusion of LUV to be used for flux measurements. LUV size was determined by quasielastic light scattering as previously described (Donovan, Benedek, and Carey, 1987; Cohen, Angelico, and Carey, 1989). Equipment included an argon ion laser (model 164, Spectra Physics, Mountain View, CA), an autocorrelator (BI-2030AT, Brookhaven Instruments, Holtsville, NY) and a thermostatically controlled sample holder. Analysis by the method of cumulants yielded mean hydrodynamic radius and polydispersity, a measure of the width of particle distribution about the mean (Mazer, Benedek, and Carey, 1980).

Fluorescence Anisotropy Measurements

LUV were incubated with 1.5 μM DPH in NaCl buffer at a probe-to-lipid molar ratio of 1:400 (Van Blitterswijk et al., 1987). Fluorescence polarization at room temperature was measured on an SLM-Aminco 500C spectrofluorometer adapted for fluoresence polarization (excitation 360 nm, emission 430 nm). Anisotropy corrected for ambient buffer fluorescence was calculated automatically using software supplied by SLM-Aminco.

Permeability Measurements

All flux measurements were performed at room temperature. For each permeability measurement, *n* refers to an individual measurement performed on an individual LUV preparation.

Water Permeability

Osmotic water permeability (P_f) was measured by monitoring self quenching of entrapped CF (Lande et al., 1994; Zeidel, Ambudkar, Smith, and Agre, 1992; Grossman et al., 1992; Priver et al., 1993; Zeidel et al., 1993). Vesicles were abruptly exposed to an osmotic gradient by rapid mixing in a stopped flow fluorimeter (SF.17MV, Applied Photophysics, Leatherhead, UK) with a measured dead time of 0.7 ms; extravesicular CF was completely quenched with antifluoroscein antibody. The excitation wavelength was 490 nm. The emission wavelength was filtered with a 515-nm cutoff filter. LUV in NaCl buffer were placed in one drive syringe, and NaCl buffer made hypertonic with the addition of sucrose was placed in the other drive syringe. Upon mixing, intravesicular CF concentration increased as water efflux occurred, leading to concentration-dependent CF quenching (see Fig. 2).

Fluorescence data from the stopped-flow device from 5–10 individual determinations were averaged and fit to a single exponential curve using software supplied by Applied Photophysics. The software utilizes a nonlinear regression (Marquardt) algorithm calculated from the time course using the Curfit routine. P_f was calculated from the time course of relative fluorescence by comparing single-exponential time constants fitted to simulated curves in which P_f was varied. Simulated curves were calculated using a commercially available software package (MathCad) from the osmotic permeability equation:

$$dV(t)/dt = (P_f)(SAV)\ (MVW)\cdot\{[C_{in}/V(t)] - C_{out}\} \quad (1)$$

where $V(t)$ is the relative volume of the vesicles at time t, P_f is osmotic water permeability, SAV is the vesicle surface area-to-volume ratio, MVW is the molar volume of water (18 cm^3/mol), and C_{in} and C_{out} are the initial concentrations of total solute inside and outside the vesicle, respectively. Because the volume within the vesicle was small compared with the volume outside, it was assumed that C_{out} remained constant throughout the experiment. Parameters from the exponential fit (amplitude and endpoint) were used to relate relative fluorescence to relative volume using boundary assumptions that relative fluorescence and volume are 1.0 at time zero and that relative volume reaches a known value (if at time zero the osmolality outside is double that inside, the relative volume reaches 0.5) at the end of the experiment.

Urea and Acetamide Permeability (P_z)

P_z was determined by monitoring relative fluorescence during efflux of permeant solute (see Fig. 3) (Zeidel et al., 1992, 1993; Lande et al., 1994; Piqueras, Somers, Hammond, Strange, Harris, Gawryl, and Zeidel, 1993; Priver et al., 1993; Chang, Hammond, Sun, and Zeidel, 1994). LUV were preequilibrated with nonelectrolyte buffer containing urea or acetamide (internal nonelectrolyte concentration 343 mM, total osmolality 560 mOsm/kg) by 30 min incubation at room temperature. Vesicles were then abruptly exposed to an equal volume of extravesicular solution containing NaCl buffer with enough sucrose added to raise the osmolality to 560 mOsm/kg, resulting in an extravesicular compartment with equal osmolality but half the nonelectrolyte concentration compared to the intravesicular compartment. Initial conditions as the two solutions were mixed were 343 mOsm permeant solute and 217 impermeant solute inside the vesicle and 171.5 mOsm permeant solute and 388.5 mOsm impermeant solute outside the vesicle. Nonelectrolyte effluxed down its concentration gradient, leading to water efflux and CF self quenching. The general formula defining solute flux across a membrane is:

$$J_z = dz/dt = (P_z)(SA)(\Delta C) \tag{2}$$

where J_z is the flux of the permeant solute z, P_z is the permeability of the permeant solute z, SA is the surface area of the vesicle, and ΔC is the difference in concentration of permeant solute inside and outside the vesicle. If

$$V_{rel} = V(t)/V_o, \tag{3}$$

where V_o is the initial volume of the vesicle and V_{rel} and $V(t)$ are the relative and absolute volumes, respectively, at time t, then for our conditions:

$$dz/dt = 560(V_o - V_o V_{rel}) \tag{4}$$

$$\Delta C = 948.5 - (777/V_{rel}) \tag{5}$$

and therefore:

$$dV_{rel}/dt = P_{urea}(SA/V_o)(1/560)(777/V_{rel} - 948.5) \tag{6}$$

By use of parameters from the single-exponential curve fit to the data, P_z was solved using MathCad.

Proton permeability (P_{H^+}). Proton permeability was determined by monitoring pH-sensitive CF quenching on the stopped-flow device (Lande et al., 1994; Piqueras et al., 1993; Chang et al., 1994; Zeidel, Nielsen, Smith, Ambudkar, Maunsbach, and Agre, 1994). LUV loaded with 0.1 mM CF were equilibrated with KCl buffer containing 1 μM valinomycin at pH 7.5. Vesicles were then abruptly mixed with KCl buffer containing enough HCl to lower the final extravesicular pH from 7.5 to 6.7. Stepwise reductions in the extravesicular pH led to reductions in the intravesicular pH and in the fluorescence of entrapped CF. Over the pH range used, relative fluorescence was linearly correlated with pH for all lipid compositions (data not shown). Fluorescence data from the

stopped-flow device were fit to a single exponential curve and fitting parameters were used to solve the equation for proton permeability. The general equation for P_H^+ is:

$$J_H^+ = (P_H^+)(SA)(\Delta C) = (\Delta pH/t)(BCV) \quad (7)$$

where J_H^+ is the flux of protons, P_H^+ is the proton permeability, SA is the surface area of the vesicle, ΔC is the initial difference in concentration of protons between the inside and outside of the vesicle, ΔpH is the excursion in pH when time equals $1/t$, t is the time constant of the single-exponential curve describing the change in fluorescence as a function of time, and BCV is the buffer capacity of an individual vesicle. Buffer capacity was determined using acetate steps as described (Lande et al., 1994; Piqueras et al., 1993; Chang et al., 1994; Zeidel et al., 1994).

Ammonia permeability (P_{NH3}). P_{NH3} was determined by monitoring pH-sensitive fluorescence of CF on the stopped-flow device after rapid mixing of LUV in NaCl buffer at pH 6.7–6.8 containing ammonium chloride at a final concentration of 5 mM (Lande et al., 1994; Piqueras et al., 1993; Chang et al., 1994; Zeidel et al., 1994). The small amount of NH3 present in the ammonium chloride permeates the membrane, titrates intravesicular protons, forming NH_4^+, and thereby raising intravesicular pH. The final intravesicular pH was determined from the linear correlation between relative fluorescence and pH. Using the rate of change of intravesicular pH, the final intravesicular pH, and the buffer capacity, P_{NH3} was calculated.

RESULTS

Anisotropy Measurements

As shown in Fig. 1 and listed in Table I, the eight lipid compositions studied exhibited a wide range of fluidities, as represented by their anisotropies. As expected, increased acyl chain saturation and increasing cholesterol and sphingomyelin content resulted in lower averaged fluidity of the bilayer (higher anisotropy) (Van Blitterswijk et al., 1987). Importantly, the measured values resembled closely those

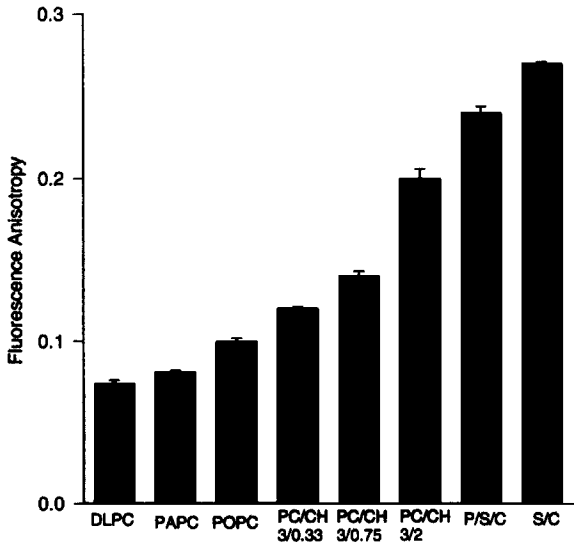

FIGURE 1. Fluorescence anisotropy of liposomes of varying lipid composition. Abbreviations as in Methods. Data represent means ± standard errors for a minimum of three different determinations.

obtained by previous investigators working with liposomes of identical compositions (Van Blitterswijk et al., 1987).

Permeability Measurements

As shown in the permeability equations above, calculation of permeabilities from flux data requires knowlege of liposome diameter, so that surface area, volume and surface area to volume ratios can be calculated. Although extrusion has been shown in numerous previous studies to provide liposomes of uniform diameter that approximate the pore size of the filters used (Hope, Bally, Webb, and Cullis, 1985), we performed measurements of liposome size using quasielastic light scattering.

TABLE I

Permeabilities Given in Centimeters per Second ± SEM

LUV population	P_f	P_{urea}	$P_{acetamide}$	P_{H+}	P_{NH3}	Anisotropy
	n	*n*	*n*	*n*	*n*	*n*
100% DLPC	$1.5 \pm 0.3 \times 10^{-2}$	$3.8 \pm 0.7 \times 10^{-6}$	$1.0 \pm 0.2 \times 10^{-4}$	$3.6 \pm 0.3 \times 10^{-1}$	$7.8 \pm 1.5 \times 10^{-2}$	$7.4 \pm 0.2 \times 10^{-2}$
	3	3	3	3	3	3
100% PAPC	$1.5 \pm 0.4 \times 10^{-2}$	$3.5 \pm 0.6 \times 10^{-6}$	$1.0 \pm 0.2 \times 10^{-4}$	$2.0 \pm 0.6 \times 10^{-1}$	ND	$8.1 \pm 0.1 \times 10^{-2}$
	3	3	3	3		4
100% POPC	$7.2 \pm 1.8 \times 10^{-3}$	$1.3 \pm 0.4 \times 10^{-6}$	$5.2 \pm 1.0 \times 10^{-5}$	$3.6 \pm 0.5 \times 10^{-1}$	$3.6 \pm 10.6 \times 10^{-2}$	$1.0 \pm 0.02 \times 10^{-1}$
	3	3	3	3	3	4
90% POPC	$3.3 \pm 1.1 \times 10^{-3}$	$4.9 \pm 0.3 \times 10^{-7}$	$3.6 \pm 1.4 \times 10^{-5}$	$1.7 \pm 0.5 \times 10^{-1}$	$4.4 \pm 0.4 \times 10^{-2}$	$1.2 \pm 0.01 \times 10^{-1}$
10% CH	3	3	3	4	4	4
80% POPC	$2.9 \pm 0.9 \times 10^{-3}$	$4.3 \pm 0.8 \times 10^{-7}$	$2.6 \pm 0.7 \times 10^{-5}$	$1.3 \pm 0.3 \times 10^{-1}$	$3.5 \pm 0.7 \times 10^{-2}$	$1.4 \pm 0.03 \times 10^{-1}$
20% CH	3	3	3	4	4	4
60% POPC	$1.3 \pm 0.5 \times 10^{-3}$	$1.2 \pm 0.3 \times 10^{-7}$	$1.3 \pm 0.3 \times 10^{-5}$	$7.6 \pm 1.8 \times 10^{-2}$	ND	$2.0 \pm 0.06 \times 10^{-1}$
40% CH	3	3	3	4		4
35% POPC	$8.5 \pm 3.9 \times 10^{-3}$	$4.4 \pm 2.5 \times 10^{-8}$	$7.9 \pm 1.9 \times 10^{-6}$	$1.1 \pm 0.3 \times 10^{-1}$	$6.8 \pm 1.3 \times 10^{-3}$	$2.0 \pm 0.06 \times 10^{-1}$
25%SPH/						
40%CH	3	3	3	4	4	4
60% SPH	$2.2 \pm 0.6 \times 10^{-4}$	$3.0 \pm 0.6 \times 10^{-9}$	$2.8 \pm 1.1 \times 10^{-6}$	ND	$2.4 \pm 0.7 \times 10^{-3}$	$2.7 \pm 0.01 \times 10^{-1}$
40% CH	3	3	3		4	4

Partition coefficients (K) are referenced in Zeidel et al. (1992*a*) and Grossman et al. (1992). Data from Priver et al. (1993).

All liposome preparations exhibited unimodal distributions of diameters ranging from 112 to 158 nm, with maximal standard errors of 3%. These diameters were used to calculate permeabilities. When selected preparations were examined by electron microscopy as previously described (Zeidel et al., 1992, 1993; Lande et al., 1994; Piqueras et al., 1993); diameters obtained by both methods were in good agreement.

Figs. 2–5 show representative examples of flux measurements of water, urea, protons, and ammonia in LUV of varying composition and fluidity. Each LUV preparation behaved as a single population in stopped-flow measurements of osmotic water efflux, nonelectrolyte efflux, H^+ influx, and NH3 influx, permitting unambiguous

calculation of permeability coefficients. In all water and small nonelectrolyte stopped-flow measurements, the final fluorescence was stable, indicating that sucrose, Na^+, and Cl^- permeation of LUV were negligible over the time scales used, and that a steady state condition had been attained. Table I summarizes the permeabilities to water, urea, acetamide, protons, and ammonia of all of the LUV populations studied. Proton permeability could not be determined for SPH/CH LUV due to a fluorescence artifact encountered during the stopped-flow experiments. It is

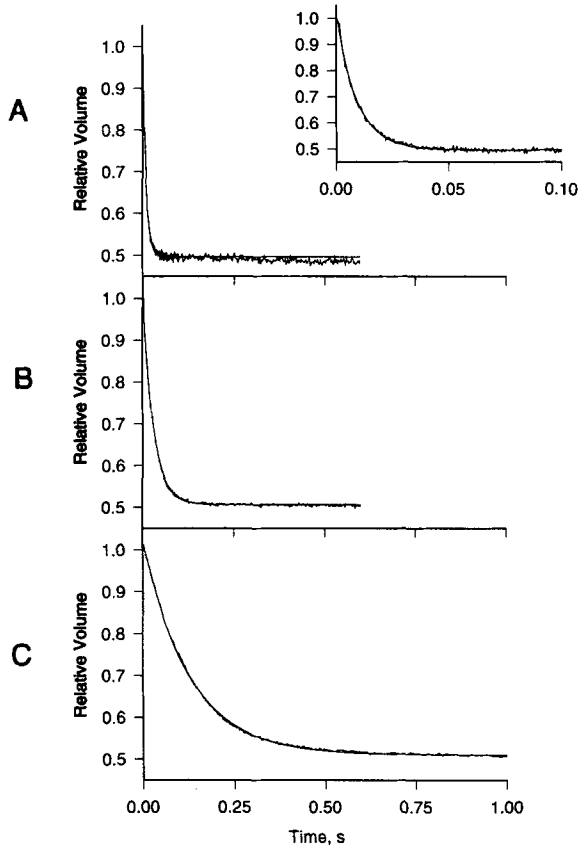

FIGURE 2. Water flux through liposomes of varying composition. (*A, inset*) DLPC. (*B*) POPC/10% cholesterol. (*C*) POPC/SPH/CHOL. Representative averaged curves and their exponential fits are shown. To compare the rates of water flux, time axes of *A–C* are identical. (*A, inset*) Expands early time course.

apparent that permeabilities to water, small nonelectrolytes, and ammonia, but not protons changed markedly as a function of fluidity.

Relation of Averaged Fluidity of the Bilayer to Permeability

Fig. 6 relates permeabilities to water, urea, acetamide, protons, and ammonia to fluorescence anisotropy. As shown in Fig. 6, *A–D*, the relation is well fit to single exponential functions ($r \geq 0.96$) for water, urea, acetamide, and ammonia. By contrast, proton permeability varies less with fluidity (Fig. 7).

The solubility diffusion model of permeability predicts that reductions in mem-

brane fluidity will reduce permeability by reducing the rate at which substances diffuse across the lipid bilayer (Finkelstein, 1986; Lieb and Stein, 1969; Stein, 1989, 1990). The relationship between measured permeability of a substance, P_s and its determinants can be expressed as:

$$P_s = (D_{mem}K)/d \tag{8}$$

where D_{mem} is the diffusion coefficient for the substance across the lipid bilayer, K is the partition coefficient in a model solvent, hexadecane, and d is the thickness of

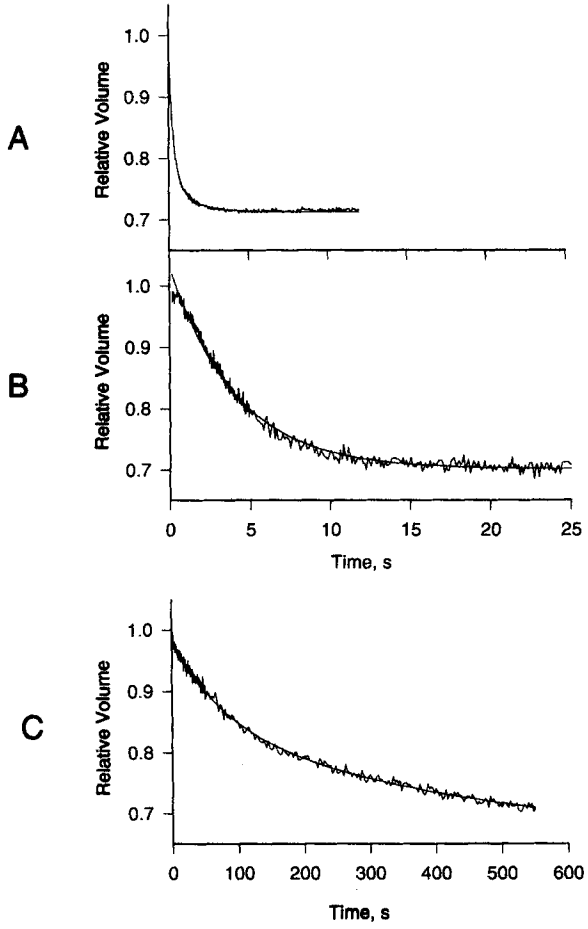

FIGURE 3. Urea flux through liposomes of varying composition. (*A*) DLPC. (*B*) POPC/10% cholesterol. (*C*) POPC/SPH/CHOL. (*A* and *B*) Identical time axes; (*C*) longer time axes.

the lipid bilayer; this thickness was assumed to be the same for all lipid compositions (Stein, 1989, 1990) and was estimated to be 50 Å, the value measured for lipid bilayers formed with egg lecithin in decane (Xiang, Chen, and Anderson, 1992). If P_s is in cm/s, and d is expressed in cm, D_{mem} is expressed in cm^2/s. Previous studies have shown that, as occurs in free solution, in lipid bilayers, the logarithm of D_{mem} is inversely related to molecular radius of the permeating substance (Stein, 1989,

1990). The molecular radius of the permeating substance provides a measure of the amount of steric hindrance the substance will encounter in crossing the lipid bilayer. From these results, we would predict that D_{mem} would be similarly related to a measure of the steric hindrance offered by the lipid bilayer to a given substance, the membrane fluidity. Fig. 8 shows the relationship between ln D_{mem} and averaged fluidity of the bilayer as reported by fluorescence anisotropy for water, urea, and

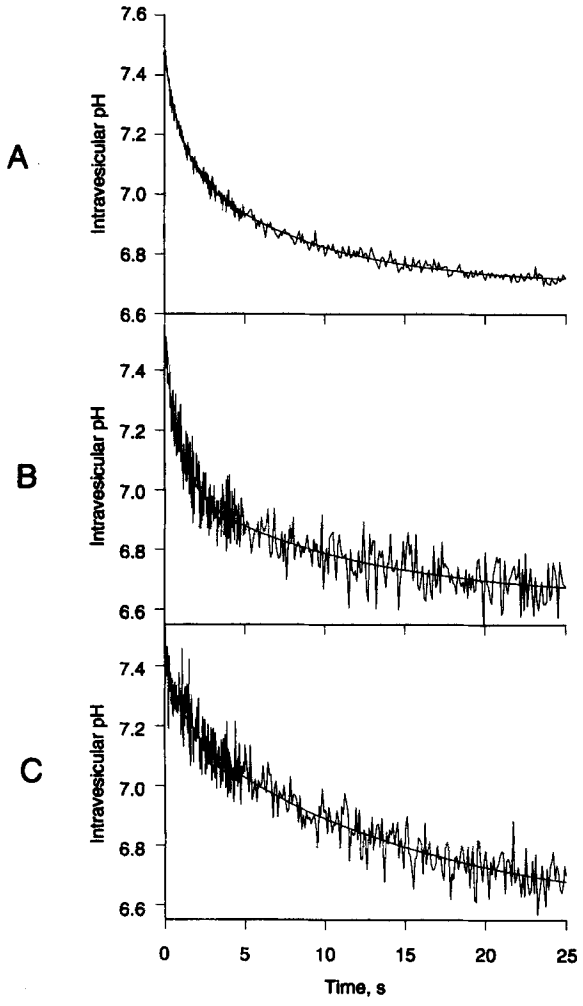

FIGURE 4. Proton flux through liposomes of varying composition. (*A*) DLPC; (*B*) POPC/405 CHOL; (*C*) POPC/SPH/CHOL. All panels have identical time axes.

acetamide permeabilities. A similar tight correlation was observed for ammonia (data not shown).

DISCUSSION

The apical membranes of several barrier epithelia, including the mammalian collecting duct and the amphibian urinary bladder in the absence of antidiuretic hor-

mone, the mammalian thick ascending limb, urinary bladder, and gastric mucosa, must withstand large concentration gradients to protect against cell damage and loss of barrier function (Kikeri et al., 1989; Harris et al., 1991; Grossman et al., 1992; Priver et al., 1993; Zeidel et al., 1993). In the absence of specific transporter proteins, substances permeate biological membranes via the lipid bilayer, so that the barrier function of these apical membranes must be defined in terms of the mechanisms by which substances permeate lipid bilayers (Finkelstein, 1986; Stein, 1989, 1990). Indeed, early studies demonstrated that simple combinations of phospholipids and cholesterol could mimic the entire range of water and urea permeabilities encountered in nature (Finkelstein, 1976*a*,*b*, 1986).

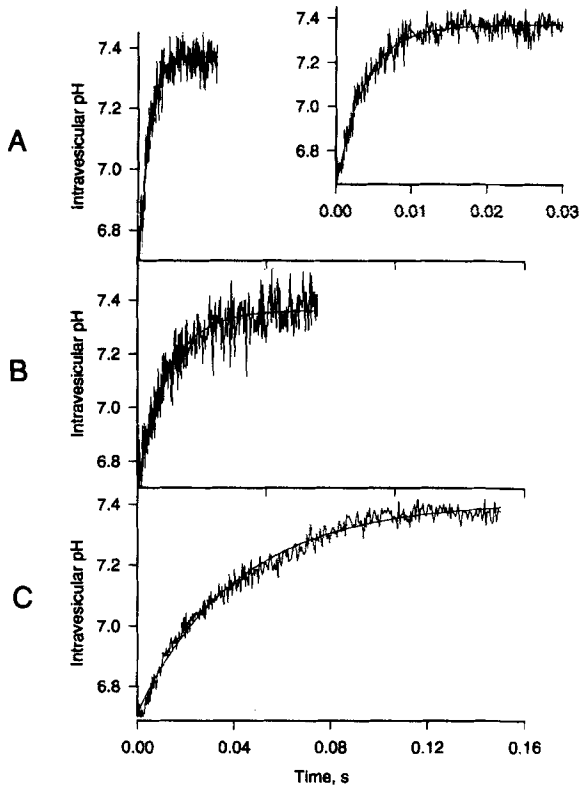

FIGURE 5. Ammonia flux through liposomes of varying composition. (*A, inset*) DLPC; (*B*) POPC/10% cholesterol; (*C*) POPC/SPH/CHOL. Time axes of *A–C* are identical. (*A, inset*) Expands early timecourse.

The solubility-diffusion model of permeation states that the permeability of a substance is determined by its oil:water partition coefficient (K) and its diffusion coefficient through bulk lipid (D_{mem}) (Finkelstein, 1986; Stein, 1989, 1990). These parameters reflect the ability of the substance both to leave the aqueous medium for the lipid of the bilayer, and to diffuse through the hydrocarbon of the bilayer, and are related to the measured permeability by Eq. 8. This model has been validated, both for artificial lipid bilayers and biological membranes by measuring the permeabilities of a wide variety of substances. The importance of the partition coefficient in determining permeability was demonstrated by the tight relationship be-

tween the logarithm of the permeability coefficient P_s and the logarithm of K for each substance (Finkelstein, 1986; Stein, 1989, 1990). The fact that several model hydrophobic substances such as olive oil, hexadecane, or ether can provide log K values which relate linearly to log P indicates that the specifics of lipid structure are not critical for defining the relationship between K and P_s (Finkelstein, 1986; Stein, 1989, 1990). The role of the diffusion of the substance through the lipid bilayer has been demonstrated by comparing the log of D_{mem}, calculated as in Eq. 8, to the mo-

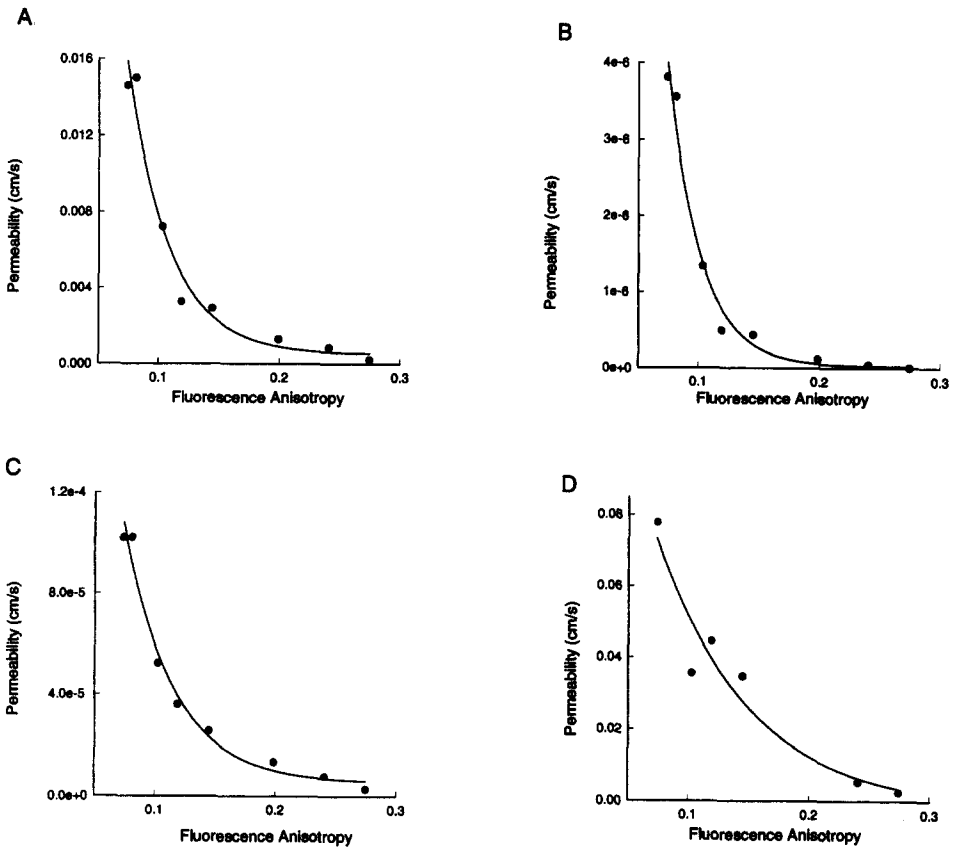

FIGURE 6. Permeabilities of different liposome preparations expressed as a function of their fluorescence anisotropy. Ordinates: permeabilities in centimeters per second. Abscissas: fluorescence anisotropy. (*A*) Water permeabilities. (*B*) Urea permeabilities. (*C*) Acetamide permeabilities. (*D*) Ammonia permeabilities. All curves are fitted single exponentials.

lecular weight of the substance (Stein, 1989, 1990). (This approach has several limitations for our results in that both the partition coefficient and the thickness of the lipid bilayer may vary with lipid composition. With respect to the thickness of the bilayer, recalculating D_{mem} using the range of thicknesses measured for artificial bilayers [30–60 Å] does not alter the linear relationship between ln and D_{mem} and anisotropy [data not shown]. The partition coefficient may vary with lipid composi-

tion and may vary along the thickness of the bilayer. However, partition coefficients for organic solvents do correlate well with permeabilities of different solutes through a variety of biological and artificial membranes, indicating that these coefficients are applicable at a macroscopic level.) These results have provided evidence that the membrane functions as a hydrophobic sieve, resembling a polymer, and retarding the flux of larger molecules to a far greater extent than that of smaller molecules. The present studies were designed to test the solubility diffusion model for a number of substances by examining the effect on permeability of varying systematically the averaged fluidity of the bilayer, as estimated by DPH anisotropy.

Membrane fluidity is defined as the inverse of viscosity, the property describing the resistance of a fluid to movement (LeGrimellec, Friedlander, El Yandouzi, Zlatkine, and M. Giocondi, 1992; Shinitzky, 1984). Most data on fluidity of biological

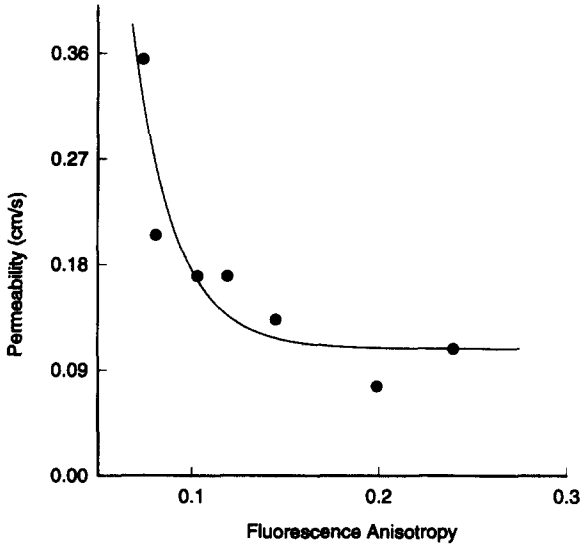

FIGURE 7. Proteon permeabilities of different liposome preparations expressed as a function of fluorescence anisotropy. A fitted single exponential curve is shown.

membranes have been obtained from the steady state fluorescence polarization of the lipophilic probe DPH, a measurement which corresponds to the lipid order of the bulk hydrocarbon (LeGrimellec et al., 1992; Shinitzky, 1984). Although newer probes are available to examine fluidities of microdomains of the lipid bilayer, such as the surface (LeGrimellec et al., 1992; Shinitzky, 1984), the potential role of fluidity in governing D_{mem} suggested that a measure of averaged fluidity of the bilayer might correlate well with D_{mem}.

While fluidity has long been advocated as a determinant of basal membrane permeability, there is little data comparing DPH anisotropy to measurements of membrane permeabilities. By contrast, numerous studies have examined the effects of changes in membrane fluidity on the activities of membrane transport proteins (LeGrimellec et al., 1992; Shinitzky, 1984; Friedlander, Shahedi, LeGrimellec, and Amiel, 1988). In early studies relating permeability to membrane physical state,

Carruthers and Melchior (1983), using microturbidimetry and differential scanning calorimetry techniques, found a transition from low to high water permeability paralleling the bilayer liquid crystalline to fluid phase transition (Carruthers and Melchior, 1983). Subsequently, Worman, Brasitus, Dudeja, Fozzard, and Field (1986), studying bovine tracheal epithelial cell apical membranes, examined the relationship between lipid fluidity and water permeability (Worman et al., 1986).

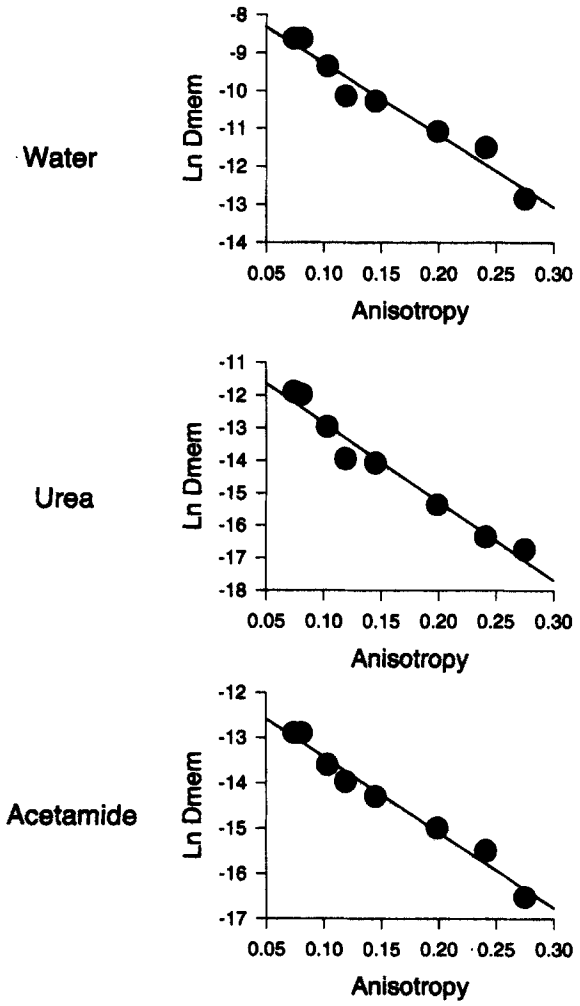

FIGURE 8. Relationship between the natural log of calculated D_{mem} and fluorescence anisotropy for water, urea, and acetamide permeabilities for the different liposome preparations. Linear fits to the data are shown.

Membranes treated with increasing concentrations of benzyl alcohol, a known fluidizer, led to concommitent increases in fluidity and relative water permeability. The relationship between relatively impermeant membranes and fluidity is less well studied. Verkman and Masur (1988), studying isolated toad bladder granules, correlated very low osmotic water permeability and high DPH anisotropy (5×10^{-4} cm/s and 0.253 at 23°C, respectively) (Verkman and Masur, 1988).

To determine the relationship between DPH anisotropy and permeabilities, several conditions must be met. First, the liposomes must be of uniform size and the size must be known. As discussed above, the flux data demonstate the presence of uniform populations of liposomes. Moreover, the reasonable expectation that the liposomes would be roughly 100 nm in diameter was confirmed by quasielastic light scattering and electron microscopy. The second important condition is that the observed fluxes reflect movement of substances across the membrane and not cross the unstirred layer of aqueous medium in contact with the membrane. Because permeability coefficients are reciprocals of resistances and the resistances of the unstirred layers and the membrane to flux are in series:

$$1/P_{tot} = 1/P_{mem} + 1/P_{US}, \quad (9)$$

where P_{tot} is the observed permeability coefficient, P_{mem} is the actual membrane permeability and P_{US} is the permeability coefficient for the unstirred layers (Stein, 1989, 1990). Several considerations indicate that P_{US} is high relative to P_{mem}, so that $1/P_{US}$ approaches 0 for all of the substances studied here. First, the measured permeabilities varied significantly with lipid composition and DPH anisotropy. Because all of the liposomes were of similar size and all were subjected to identical conditions, it can be anticipated that P_{US} would be similar under all conditions. The variability of measured permeabilities indicates that unstirred layer effects did not contribute substantially to the measured values. Second, we have previously inserted gramicidin pores and reconstituted Aquaporin CHIP into liposomes of similar size, and studied them under similar conditions (Zeidel et al., 1992, 1994). Gramicidin increased the apparent proton permeability by 50–100-fold, and aquaporin CHIP increased P_f by up to 20-fold, indicating that P_{US} was at least 20-fold higher than P_{mem} for water, and was 50–100-fold higher than P_{mem} for protons. In the case of aquaporin CHIP, the conductance of individual channels obtained in these measurements as well as the activation energy and mercurial sensitivity, matched closely the values obtained in native red blood cells, indicating that the unstirred layer effects were minimal in the liposome studies (Zeidel et al., 1992, 1994).

The present studies investigate directly the influence of averaged fluidity of the bilayer on membrane permeability by comparing permeabilities of a series of eight artificial lipid membranes exhibiting a wide range of DPH anisotropies normally encountered in biological membranes. Permeabilities to water, urea, and acetamide (solutes with distinctly different oil:water partition coefficients), ammonia, and protons were measured. POPC/SPH/CH and SPH/CH LUV exhibited anisotropies similar to the highest values measured in epithelial apical membranes. Furthermore, osmotic water permeabilities of POPC/SPH/CH and SPH/CH LUV (8.5×10^{-4} and 2.2×10^{-4} cm/s, respectively) were strikingly similar to values previously measured in water-tight apical epithelial membranes (Kikeri et al., 1989; Harris et al., 1991; Grossman et al., 1992; Priver et al., 1993; Zeidel et al., 1993). As shown in Fig. 6, *A–D*, the relationship between DPH anisotropy and permeabilities to water, urea, acetamide, and ammonia was well fit in each instance by single exponential functions, with higher anisotropy (lower fluidity) corresponding to lower permeability. Therefore, membrane fluidity, as indicated by DPH anisotropy ap-

pears to determine permeability to most substances. Previous studies of artificial lipid membranes showed that increasing amounts of cholesterol, sphingomyelin, and acyl chain saturation were associated with both decreased permeabilities to water and solutes and decreased fluidity (Finkelstein, 1986) The present studies demonstrate that the effects of changes in membrane composition on permeability are accounted for by the measured effects on fluidity as reported by DPH anisotropy. As shown in Fig. 8, where it was possible to calculate D_{mem}, it correlated extremely well with anisotropy, indicating that fluidity governs permeability by determining the diffusion coefficient for substances through the bilayer.

Over the range of anisotropies tested, permeabilities to water, urea, acetamide, and ammonia varied 67-, 1,290-, 36-, and 32-fold, respectively. Although the correlation between DPH anisotropy and permeability was tight, the larger effect of fluidity on urea permeability is striking. This increased range of permeabilities could be due to a larger effect of fluidity on D_{mem}. However, examining the values for D_{mem} shown in Fig. 8, the range of D_{mem}'s calculated for water, urea, and acetamide permeabilities is roughly similar, with the range being somewhat larger for urea than for the other substances. Moreover, the values for D_{mem} for urea and acetamide in bilayers of identical composition are quite similar. These results suggest that urea diffusion through the bilayer is impeded to a similar degree as acetamide. From Eq. 8, the very low urea partition coefficient amplifies the modest increase in range of urea D_{mem} values so that the range of urea permeabilities is large.

In addition to its effects on fluidity, addition of cholesterol to the bilayers might be expected to alter the packing of the polar head groups of the phospholipid molecules and to reduce the concentrations of water within the bilayer (Parasassi, Di-Stefano, Loiero, Ravagnan, and Gratton, 1994). These effects on packing and water content might or might not vary consistently with fluorescence anisotropy. However, the close relationship between D_{mem} and fluorescence anisotropy suggests that these other effects may be of secondary importance.

By contrast, proton permeability was only weakly influenced by averaged fluidity of the bilayer, varying only threefold over the range of fluidity tested (Figs. 5 and 7). These apparently anomalous results for proton permeability suggest that transmembrane proton flux occurs in a manner distinct from the flux of other substances. These data are consistent with previous studies which have demonstrated aberrantly high proton permeabilities in both artificial and biological membranes compared with other biologically relevant cations (Nagle, 1987; Gutknecht, 1987*b*; Deamer, 1987; Deamer and Nichols, 1989; Verkman and Ives, 1986). The proton permeabilities reported in these studies have varied widely, ranging from 10^{-9} to 10^{-1} cm/s. Importantly, proton fluxes are far higher in all reports than those of other ions. The cause of anomalously high proton flux is unknown. It has been suggested that protons move along hydrogen-bonded clusters of water molecules dissolved in the hydrophobic core of the lipid bilayer (water wires) (Deamer and Nichols, 1989; Nagle, 1987). Alternatively, protons may cross membranes in the form of protonated weak acids or free fatty acids in the hydrophobic core may act as protonophores, transporting protons across the membrane (Gutknecht, 1987*a*,*b*; Deamer and Nichols, 1989).

Epithelia separate compartments of widely differing composition, and apical

membranes form the major barrier to flux of water, protons, and small nonelectrolytes. Knowledge of the relationship between lipid bilayer fluidity and permeability is essential to the understanding of apical membrane barrier function. The solubility diffusion model suggests that solutes may permeate the membrane via small aqueous filled cavities that form transiently in the bilayer structure. Recent studies have defined different microdomains of the bilayer, including the interface between phospholipid headgroups and the aqueous medium, the portion of the hydrocarbon chains adjacent to the headgroups, and the portion of the hydrocarbon chains which are far from the headgroups. Studies of permeability in artificial bilayers indicate that the portion of the hydrocarbon chains adjacent to the headgroups is the likely site of the bilayer permeability barrier, selecting for solutes on the basis of partition coefficients, and acting as the major barrier to diffusion (Xiang et al., 1992). Modeling of the bilayer indicates that the region of the hydrocarbon chains adjacent to the phospholipid headgroups exhibits lower fluidity and therefore less likelihood of forming aqueous cavities than other domains of the bilayer (Xiang, 1993). These results suggest that reduced bulk fluidity of membranes may be reflected in reduced ability of the hydrocarbon chains adjacent to the phospholipid headgroups to form aqueous cavities, leading to reduced ability of solutes to permeate the membrane. The results of this study showing a tight correlation between averaged fluidity of the bilayer as estimated by DPH anisotropy and permeability for all substances studied except protons certainly agrees with this formulation.

Because apical membranes exhibit lower permeabilities than basolateral membranes, and because the cytoplasmic leaflet mixes freely between the two domains while the exofacial domain does not, it is likely that the low permeability of the apical membrane is a property of the exofacial leaflet (van Meer, Stelzer, Wijnaendts-van-Resandt, and Simons, 1987; Simons and van Meer, 1988; Bomsel, Prydz, Parton, Gruenberg, and Simons, 1989). Interestingly, it has been shown that apical membranes demonstrate transmembrane bilayer asymmetry, with exofacial leaflets containing a higher proportion of sphingomyelin and glycosphingolipids (LeGrimellec et al., 1992; Harris et al., 1991; Zeidel et al., 1993). Such a lipid composition would be expected to lower exofacial leaflet fluidity, thereby lowering permeability. Recent studies from our laboratory have provided evidence that this asymmetry in composition and fluidity may play a critical role in reducing membrane permeability (Lande et al., 1994). Whether lower fluidity in a membrane leaflet results in a reduction in the D_{mem} of the bilayer remains unclear. Further studies will be needed to determine the role of bilayer asymmetry and membrane proteins in determining the unique permeability properties of barrier epithelial apical membranes.

We thank Audrey Jackson for technical assistance and Kevin Strange, Alan Finkelstein, and H. William Harris, Jr. for helpful discussions.

M. B. Lande was supported by an NIH training grant. J. M. Donovan was the recipient of Merit Review and Research Associate Career Development Awards from the Department of Veterans Affairs. M. L. Zeidel was the recipient of a Clinical Investigator Career Development Award from the Department of Veterans Affairs. This work was supported by NIH RO-1 DK 43955 and DK 48217.

Original version received 5 October 1994 and accepted version received 22 February 1995.

REFERENCES

Bomsel, M., K. Prydz, R. G. Parton, J. Gruenberg, and K. Simons. 1989. Endocytosis in filter-grown Madin-Darby canine kidney cells. *Journal of Cell Biology.* 109:3243–3258.

Carruthers, A., and D. L. Melchior. 1983. Studies of the relationship between bilayer water permeability and bilayer physical state. *Biochemistry.* 22:5797–5807.

Chang, A., T. G. Hammond, T. T. Sun, and M. L. Zeidel. 1994. Permeability properties of the mammalian bladder apical membrane. *American Journal of Physiology.* 267:C1483–C1492.

Cohen, D. E., M. Angelico, and M. C. Carey. 1989. Quasielastic light scattering evidence for vesicular secretion of biliary lipids. *American Journal of Physiology.* 257:G1–G8.

Deamer, D. W. 1987. Proton permeation of lipid bilayers. *Journal of Bioenergetics and Biomembranes.* 19: 457–479.

Deamer, D. W., and J. W. Nichols. 1989. Proton flux mechanisms in model and biological membranes. *Journal of Membrane Biology.* 107:91–103.

Donovan, J. M., G. B. Benedek, and M. C. Carey. 1987. Self-association of human apolipoproteins A-1 and A-2 and interactions of apolipoprotein A-1 with bile salts: quasielastic light scattering studies. *Biochemistry.* 26:8116–8125.

Finkelstein, A. 1976. Water and nonelectrolyte permeability of lipid bilayer membranes. *Journal of General Physiology.* 68:127–135.

Finkelstein, A. 1986. Water Movement through Lipid Bilayers, Pores and Plasma Membranes, Theory and Reality. John Wiley and Sons, Inc., NY. XXX pp.

Friedlander, G., M. Shahedi, C. LeGrimellec, and C. Amiel. 1988. Increase in membrane fluidity and opening of tight junctions have similar effects on sodium-coupled uptakes in renal epithelial cells. *Journal of Biological Chemistry.* 263:11183–11188.

Grossman, E. B., H. W. Harris, R. A. Star, and M. L. Zeidel. 1992. Water and nonelectrolyte permeabilities of highly purified apical membranes of toad urinary bladder granular cells. *American Journal of Physiology.* 262:C1109–C1118.

Gutknecht, J. 1987*a*. Proton/hydroxide conductance and permeability through phospholipid bilayers. *Proceedings of the National Academy of Sciences, USA.* 84:6443–6556.

Gutknecht, J. 1987*b*. Proton conductance through phospholipid bilayers: water wires or weak acids? *Journal of Bioenergetics and Biomembranes.* 19:427–441.

Harris, H. W., D. Kikeri, A. Janoshazi, A. K. Solomon, and M. L. Zeidel. 1990. High proton flux through membranes containing antidiuretic hormone water channels. *American Journal of Physiology.* 259:F366–F371.

Harris, H. W. J., K. Strange, and M. L. Zeidel. 1991. Current understanding of the cellular biology and molecular structure of the antidiuretic hormone-stimulated water transport pathway. *Journal of Clinical Investigation.* 88:1–8.

Hope, M. J., M. B. Bally, G. Webb, and P. R. Cullis. 1985. Production of large unilamellar vesicles by a rapid extrusion procedure. Characterization of size distribution, trapped volume and ability to maintain a membrane potential. *Biochimica et Biophysica Acta.* 812:55–65.

Kikeri, D., A. Sun, M. L. Zeidel, and S. C. Hebert. 1989. Cell membranes impermeable to NH3. *Nature.* 339:478–480.

Lande, M. B., N. A. Priver, and M. L. Zeidel. 1994. Determinants of apical membrane permeabilities of barrier epithelia. *American Journal of Physiology.* 267:C367–C374.

LeGrimellec, C., G. Friedlander, E. H. El Yandouzi, P. Zlatkine, and M. Giocondi. 1992. Membrane fluidity and transport properties in epithelia. *Kidney International.* 42:825–836.

Lieb, W. R., and W. D. Stein. 1969. Biological membranes behave as non-porous polymeric sheets with respect to the diffusion of non-electrolytes. *Nature.* 224:240–243.

Mazer, N. A., G. B. Benedek, and M. C. Carey. 1980. Quasielastic light scattering studies of aqueous biliary lipid systems. Mixed micelle formation in bile salt-lecithin solutions. *Biochemistry.* 19:601–615.

Nagle, J. F. 1987. Theory of passive proton conductance in lipid bilayers. *Journal of Bioenergetics and Biomembranes.* 19:413–426.

Nichols, J. W., and D. W. Deamer. 1980. Net proton-hydroxyl permeability of large unilamellar liposomes measured by an acid-base titration technique. *Proceedings of the National Academy of Sciences, USA.* 77:2038–2042.

Parasassi, T., M. DiStefano, M. Loiero, G. Ravagnan, and E. Gratton. 1994. Cholesterol modifies water concentration and dynamics in phsopholipid bilayers: a fluorescence study using laurdan probe. *Biophysical Journal.* 66:763–768.

Piqueras, A. I., M. Somers, T. G. Hammond, K. Strange, H. W. Harris, M. Gawryl, and M. L. Zeidel. 1993. Permeability properties of rat renal lysosomes. *American Journal of Physiology.* 266:C121–C133.

Priver, N. A., E. C. Rabon, and M.L. Zeidel. 1993. Apical membrane of the gastric parietal cell: water, proton, and nonelectrolyte permeabilities. *Biochemistry.* 32:2459–2468.

Shinitzky, M. 1984. Physiology of Membrane Fluidity. CRC Press, Boca Raton, FL.

Simons, K., and G. van Meer. 1988. Lipid sorting in epithelial cells. *Biochemistry.* 27:6197–6202.

Stein, W. D. 1989. Transport and Diffusion across Cell Membranes. Academic Press, NY.

Stein, W. D. 1990. Channels, Carriers, and Pumps. An Introduction to Membrane Transport. Academic Press, San Diego, CA.

Van Blitterswijk, W. J., B. W. Van Der Meer, and H. Hilkmann. 1987. Quantitative contributions of cholesterol and the individual classes of phospholipids and their degree of fatty acyl unsaturation to membrane fluidity measured by fluorescence polarization. *Biochemistry.* 26:1746–1756.

van Meer, G., E. H. K. Stelzer, W. Wijnaendts-van-Resandt, and K. Simons. 1987. Sorting of sphingolipids in epithelial (Madin-Darby) canine kidney cells. *Journal of Cell Biology.* 105:1623–1635.

Verkman, A. S., and H. E. Ives. 1986. Anomalous driving force for renal brush border H^+/OH^- transport characterized by using 6-carboxyfluorescein. *Biochemistry.* 25:2876–2882.

Verkman, A. S., and S. K. Masur. 1988. Very low osmotic water permeability and membrane fluidity in isolated toad bladder granules. *Journal of Membrane Biology.* 104:241–251.

Worman, H. J., T. A. Brasitus, P. K. Dudeja, H. A. Fozzard, and M. Field. 1986. Relationship between lipid fluidity and water permeability of bovine tracheal epithelial cell apical membranes. *Biochemistry.* 25:1549–1555.

Xiang, T.-X. 1993. A computer simulation of free volume distributions and related structural properties in a model lipid bilayer. *Biophysical Journal.* 65:1108–1120.

Xiang, T.-X., X. Chen, and B. D. Anderson. 1992. Transport methods for probing the barrier domain of lipid bilayer membranes. *Biophysical Journal.* 63:78–88.

Yuli, I., W. Wilbrandt, and M. Shinitzky. 1981. Glucose transport through cell membranes of modified lipid fluidity. *Biochemistry.* 20:4250–4256.

Zeidel, M. L., S. Ambudkar, B. Smith, and P. Agre. 1992. Reconstitution of functional water channels in liposomes containing purified red cell CHIP28 protein. *Biochemistry.* 31:7436–7440.

Zeidel, M. L., S. Nielsen, B. L. Smith, S. V. Ambudkar, A. B. Maunsbach, and P. Agre. 1994. Ultrastructure, pharmacologic inhibition, and transport selectivity of Aquaporin CHIP in proteoliposomes. *Biochemistry.* 33:1606–1615.

Zeidel, M. L., K. Strange, F. Emma, and H. W. Harris, Jr. 1993. Mechanisms and regulation of water transport in the kidney. *Seminars in Nephrology.* 13:155–167.